

Figure S1

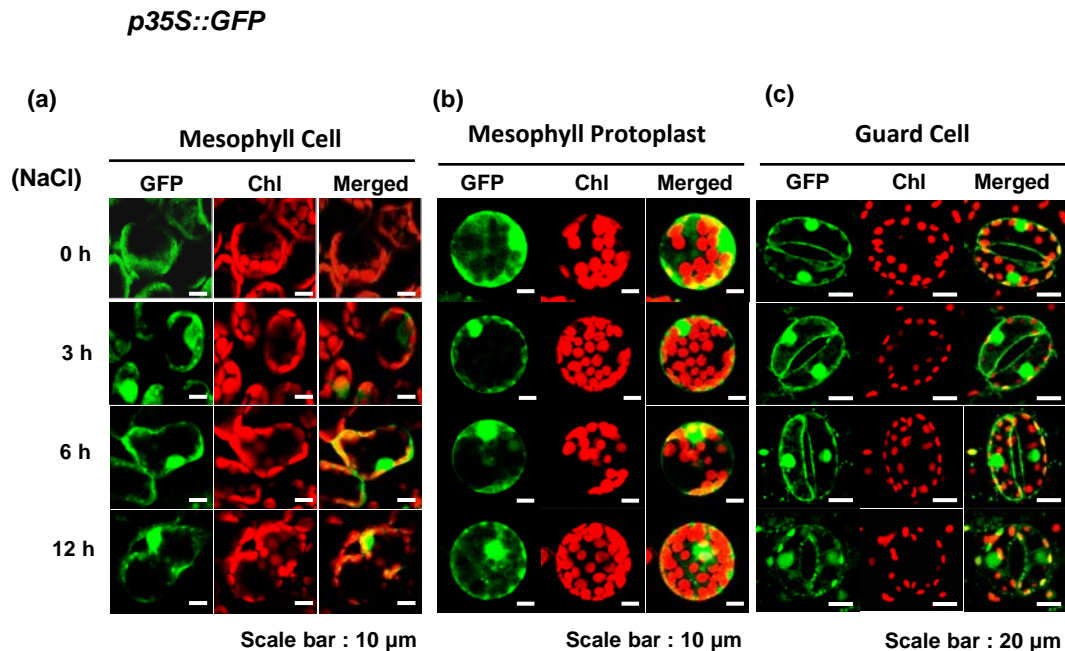


Figure S1. Green fluorescent protein (GFP) fluorescence localization and immunoblot analysis in the cellular compartments of *p35S::GFP* transgenic plants under salt stress. (a–c) Confocal laser scanning microscopy (CLSM) images of (green) GFP fluorescence were observed in (a) mesophyll cells, (b) mesophyll protoplasts, and (c) guard cells of 6-week-old plants exposed to salt stress with 200 mM NaCl. CLSM images of (green) GFP fluorescence and (red) chlorophyll autofluorescence from chloroplasts are merged in the third column.

Figure S2

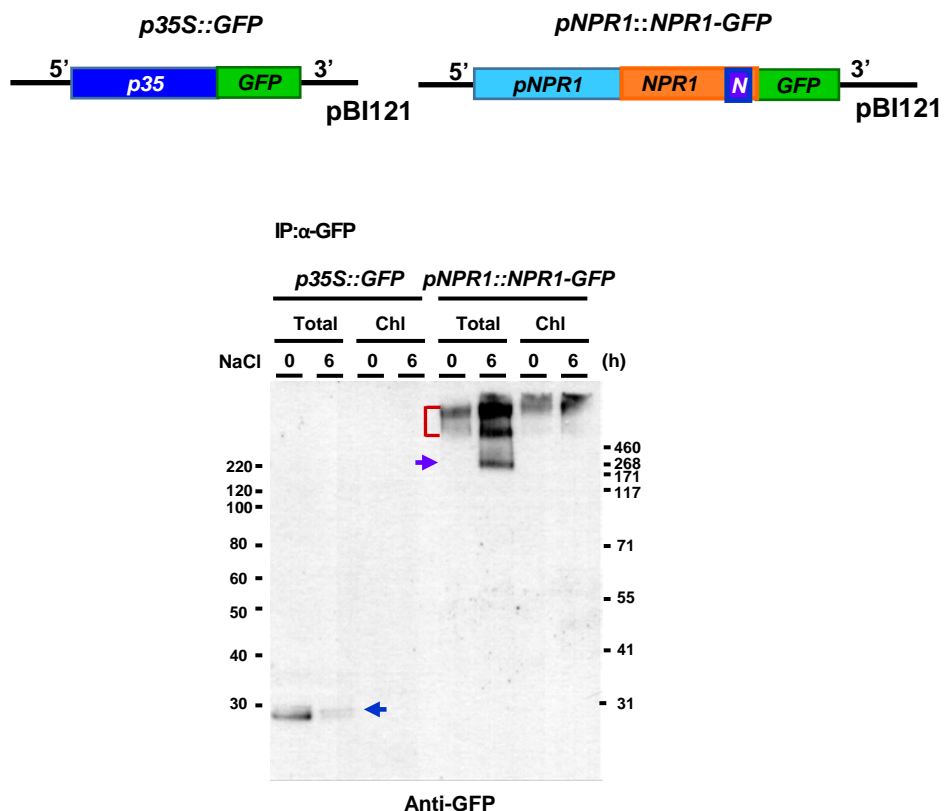


Figure S2. Immunoblots of the total and chloroplast protein fractions from *pNPR1::NPR1-GFP* under salt stress. After immunoprecipitating the protein fractions using GFP-Trap agarose, western blotting with anti-GFP antibody was performed. GFP-tagged nonexpressor of pathogenesis-related gene 1 (NPR1-GFP) oligomer (high molecular weight) and dimer (low molecular weight) are indicated with red square brackets. Purple arrow indicates GFP dimer. Blue arrow indicates GFP only in total protein fraction in *p35S::GFP* transformants.

Figure S3

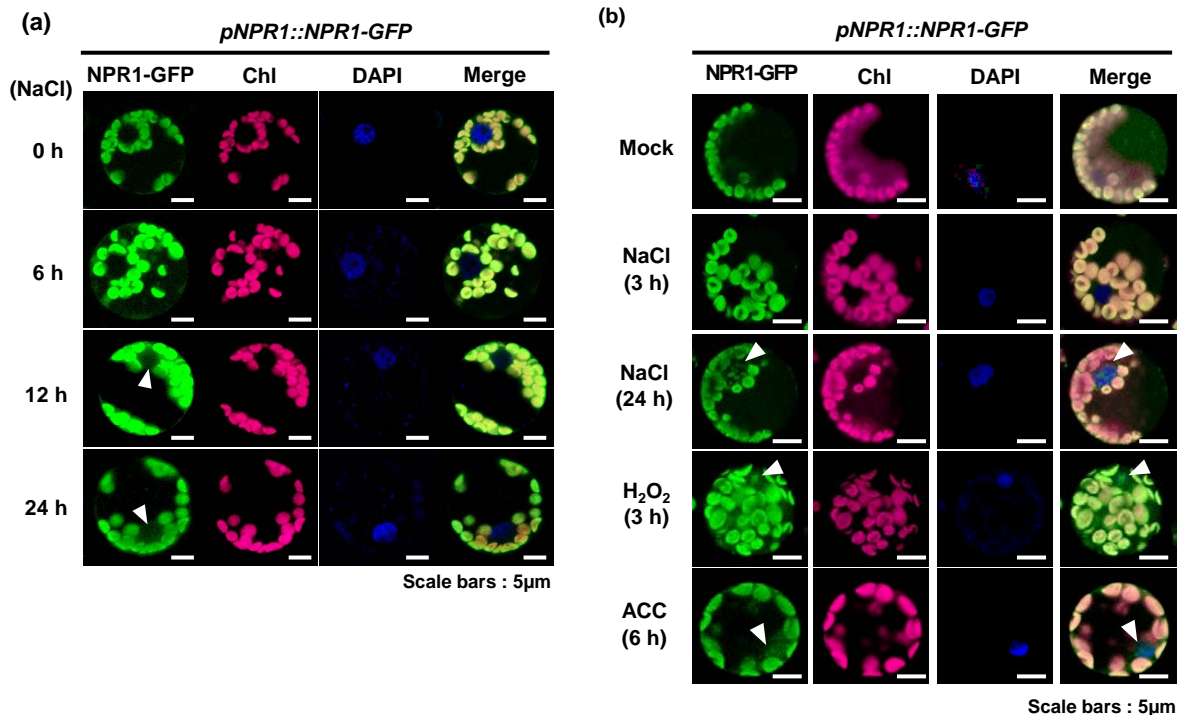


Figure S3. CLSM images of GFP fluorescence on mesophyll protoplasts after treatments with salt stress, H_2O_2 or ACC. **(a)** CLSM images of GFP fluorescence in mesophyll protoplasts from 6-week-old *pNPR1::NPR1-GFP* transgenic plants exposed to salt stress using 200 mM NaCl. **(b)** CLSM images of GFP fluorescence in mesophyll protoplasts from *pNPR1::NPR1-GFP* transgenic plants treated with 200 mM NaCl, 5 mM H_2O_2 , or 1 mM 1-amino-1-cyclopropane carboxylic acid (ACC). Images of (green) GFP fluorescence and (magenta) chlorophyll autofluorescence from chloroplasts are merged in the fourth column. DAPI staining (blue) images are presented in the third column.

Figure S4

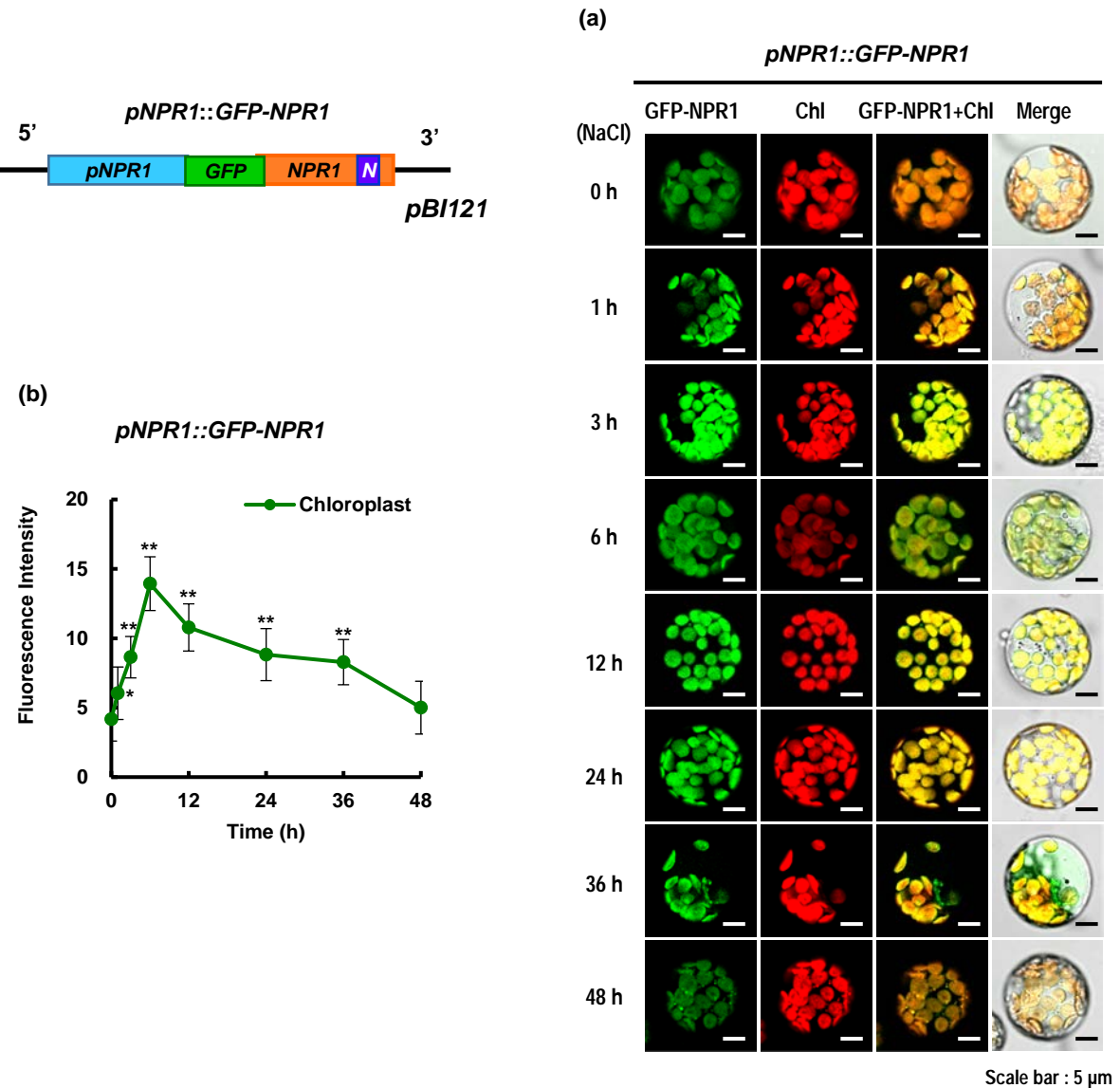


Figure S4. NPR1-GFP localization in salt stress. (a) GFP fluorescence localization in cellular compartments of mesophyll protoplasts after transient expression with *pNPR1::NPR1-GFP* construct. Confocal laser scanning microscopy (CLSM) images of (green) GFP fluorescence and (red) chlorophyll autofluorescence from chloroplasts are merged in the third column. The bright-field image is merged into the fourth column. (b) GFP intensity was quantified in the chloroplasts after transient *pNPR1::NPR1-GFP* (green line) expression under salt stress ($n=30$). Data are expressed as mean \pm SD. An asterisk indicates a significant difference from 0 h (one asterisk ($P<0.05$) or two asterisks ($P < 0.01$)).

Figure S5

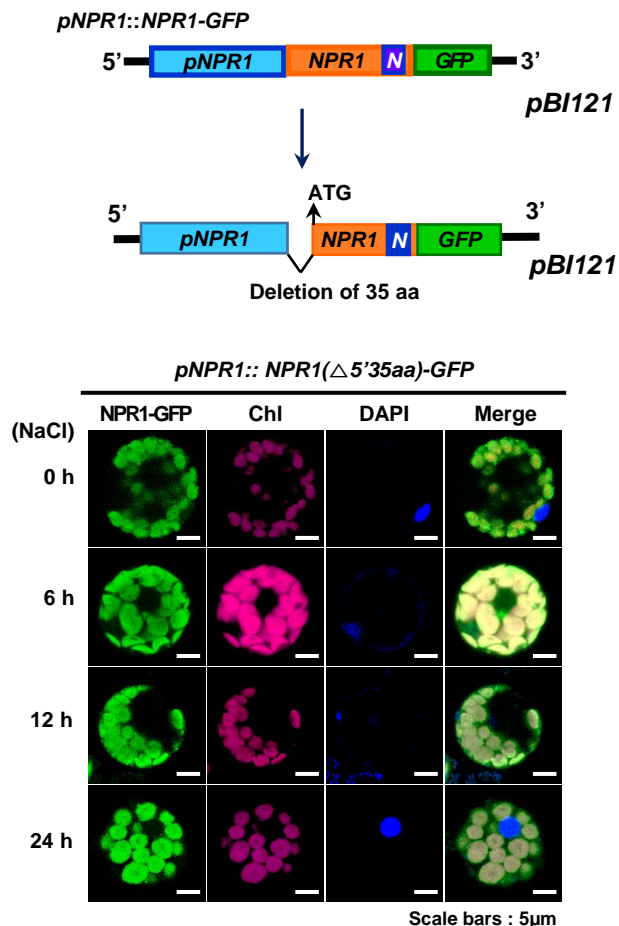


Figure S5. Subcellular localization of *NPR1(Δ5'35aa)-GFP*. GFP-tagged nonexpressor of pathogenesis-related genes 1 (GFP–NPR1) localization in intracellular compartments of mesophyll protoplasts after transient *pNPR1::NPR1(Δ5'35aa)-GFP* expression. After deleting the N-terminal 35 amino acids from the *NPR1* open reading frame, a deletion construct with the ATG start codon was constructed. GFP fluorescence localization in mesophyll protoplasts after transient *pNPR1::NPR1(Δ5'35aa)-GFP* construct expression. Confocal laser scanning microscopy (CLSM) images of (green) GFP fluorescence and (magenta) chlorophyll autofluorescence from chloroplasts are merged in the third column. The bright-field image is merged into the fourth column. Scale bars = 5 μm.

Figure S6

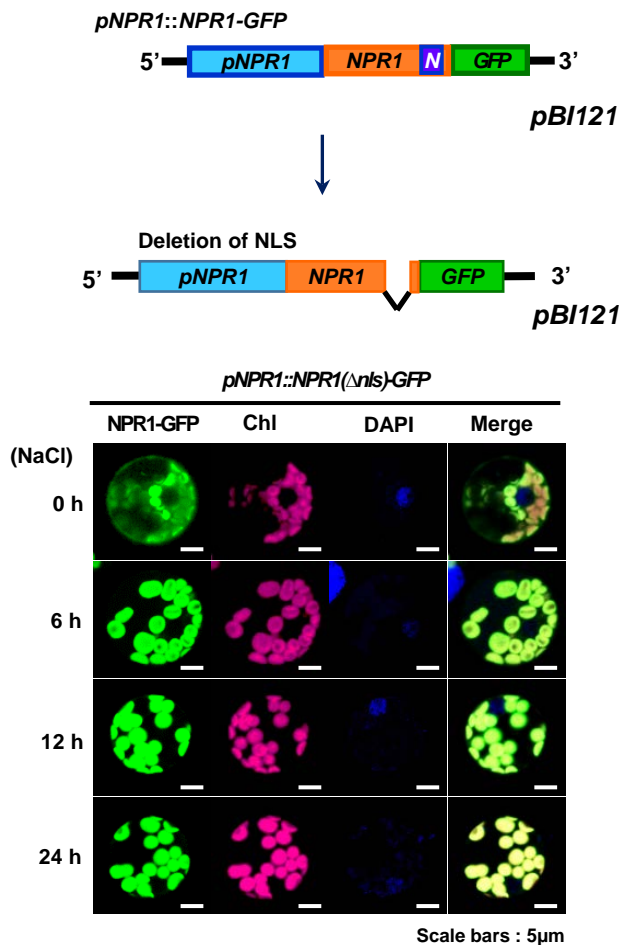


Figure S6. Subcellular localization of nuclear localization signal (NLS)-deleted NPR1-GFP mutant. **(a)** Deletion constructs of the NLS within the NPR1 open reading frame were subcloned in frame with a C-terminal GFP and under the control of native NPR1 promoter. NLS-deleted constructs were transiently expressed in mesophyll protoplast of wild-type (WT) tobacco plants. **(b)** CLSM images of GFP fluorescence in mesophyll protoplasts from plants transiently expressing *pNPR1::NPR1(Δ NLS)-GFP* under salt stress. Images of (green) GFP fluorescence and (magenta) chlorophyll autofluorescence are merged in the fourth column. DAPI staining (blue) images are presented in the third column. N indicates NLS.

Figure S7



NtNPR1 LSS-CSSSRGNDK NK PFK --- 588
 AtNPR1 TDGSTSKSTGGRSNRKLSHRRR --- 593
 CaNPR1 VSS-CSSSRGNDK NK PFK --- 582
 VvNPR1 -SS-SSSSTSLPGRNNRLSCK --- 584
 TcNPR1 SS-SSSSISIIVGRNGKLTGSGRRG 591
 OsNPR1 -SS-SSSSTSIACIRRR --- 582
 AtNPR3 SA-SSSPSRSSRDLNNTT ----- 586
 AtNPR4 SSSSPA--SSSLREALNP --- 574
 GmNPR1 SSSSS-SSSLRDSVVVHYKARKV --- 590
 MhNPR1 PSSSE-S-TSPKKIGANQKVREP --- 586

Figure S7. Alignment of nonexpressor of pathogenesis-related genes 1 (NPR1) proteins from different plant species: *Nicotiana tabacum* (NtNPR1, KY402167), *Arabidopsis thaliana* (AtNPR1, ATU76707; AtNPR3, NM_123879.3; AtNPR4, AY785951), *Theobroma cacao* (TcNPR1, HM117159), *Oryza sativa* (Japonica cultivar-group) (OsNPR1, DQ450948), *Glycine max* (GmNPR1, NM001251729), *Capsicum annuum* (CaNPR1, DQ648785), *Vitis vinifera* (VvNPR1, XM002281439), and *Malus hupehensis* (MhNPR1, FJ598141). Two conserved protein–protein interaction motifs, a broad complex, tramtrack, bric a brac/poxvirus and zinc-finger (BTB/POZ)-like domain (pink bar), and an ankyrin-repeat domain (purple bar) are indicated. Nuclear localization signal is indicated with asterisks and a green open box. Two cysteines (Cys521 and Cys529) required for salicylic acid (SA)-dependent transcriptional activation in *Arabidopsis* are indicated in uppercase C in red. The putative NIMIN1 and NIMIN2 binding regions are indicated with asterisks and a black open box. The SA-binding region is indicated with asterisks and a red open box. Specific amino acids playing important roles in SA binding are indicated with red arrows. The conserved region (VDLNE) of ethylene-responsive element binding factor-associated amphipathic repression motif is indicated with a blue bracket. Red box (■) in *Arabidopsis* NPR1 C156 indicates the redox sensor for oligomerization.

Figure S8

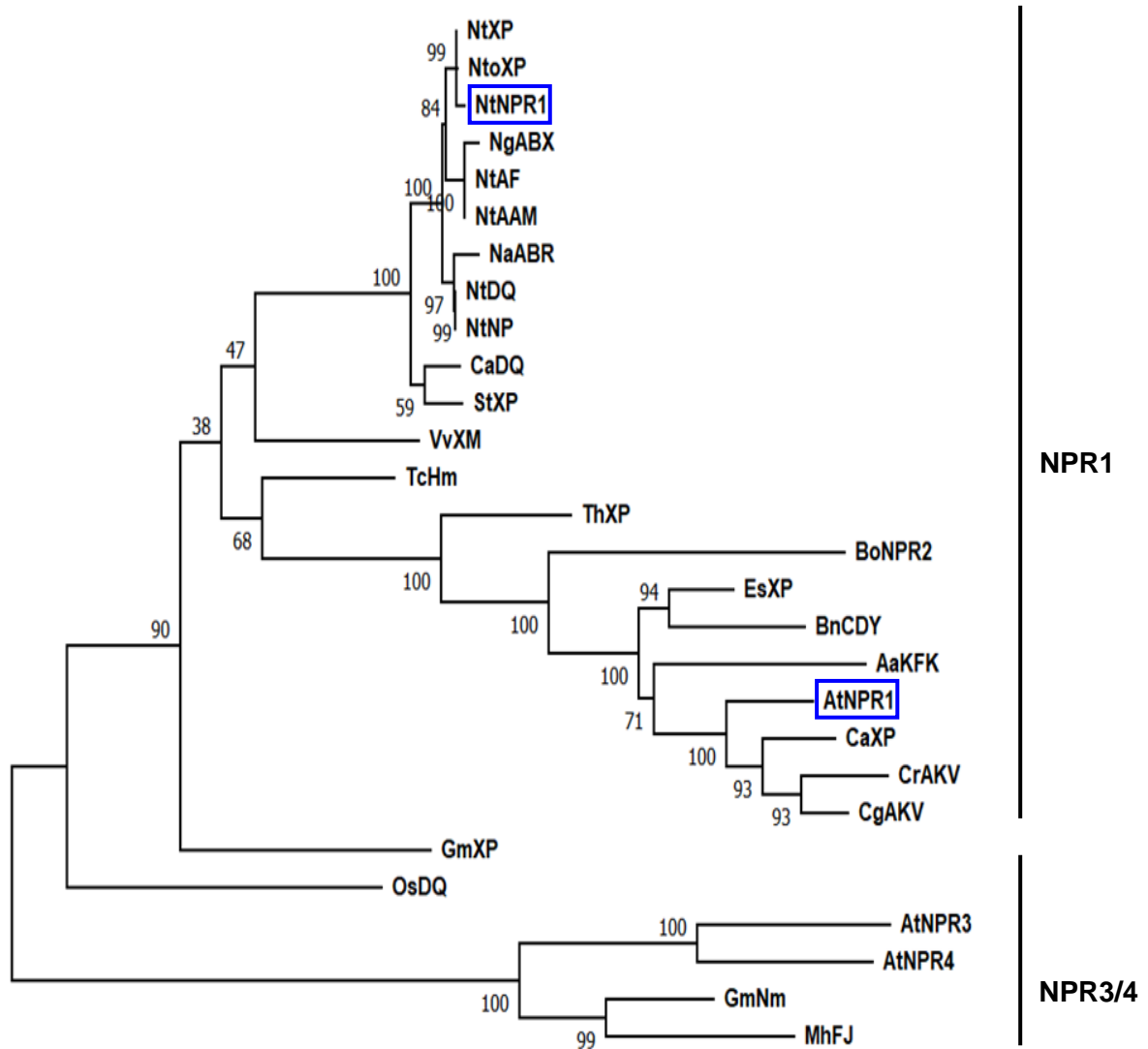


Figure S8. Phylogenetic tree constructed using the neighbor-joining method in MEGA version 11.0 based on the sequences of 28 NPR1 genes from different plants species. Amino acid sequence of each protein was downloaded from NCBI. Each number at nodes is the percentage of 1,000 bootstrap replicate support. Abbreviations and GenBank accession numbers are presented in parentheses after the species name: *Nicotiana tabacum* (NtNPR1, KY402167; NtAF, AF480488; NtAAM, AAM62410.1; NtXP, XP_016503804; NtNP, DQ837218.1 and NtDQ, DQ837218), *Nicotiana glutinosa* (NgABX, ABX71071.1), *Nicotiana tomentosiformis* (NtoXP, XP_009606361), *Nicotiana attenuata* (NaABR, ABR23001.1), *Solanum tuberosum* (StXP, XM_006357647), *Arabidopsis thaliana* (AtNPR1, ATU76707; AtNPR3, NM_123879.3: AtNPR4, AY785951), *Theobroma cacao* (TcHM, HM117159), *Oryza sativa* (japonica cultivar-group) (OsDQ, DQ450948), *Glycine max* (GmNM, NM001251729; GmXP, XP_003534926), *Capsicum annuum* (CaDQ, DQ648785), *Vitis vinifera* (VvXM, XM002281439), *Camelina sativa* (CaXP, XP_010430551), *Capsella rubella* (CrAKV, AKV91676.1), *Capsella grandiflora* (CgAKV, AKV91675.1), *Eutrema salsugineum* (EsXP, XP_006391648.1), *Brassica napus* (BnCDY, CDY34413.1), *Arabis alpine* (AaKFK, KFK36581.1), *Tarenaya hassleriana* (ThXP, XP_010545358.1), *Brassica oleracea* var. *oleracea* (BoNPR2, XM_013780436), and *Malus hupehensis* (MhFJ, FJ598141).

Figure S9

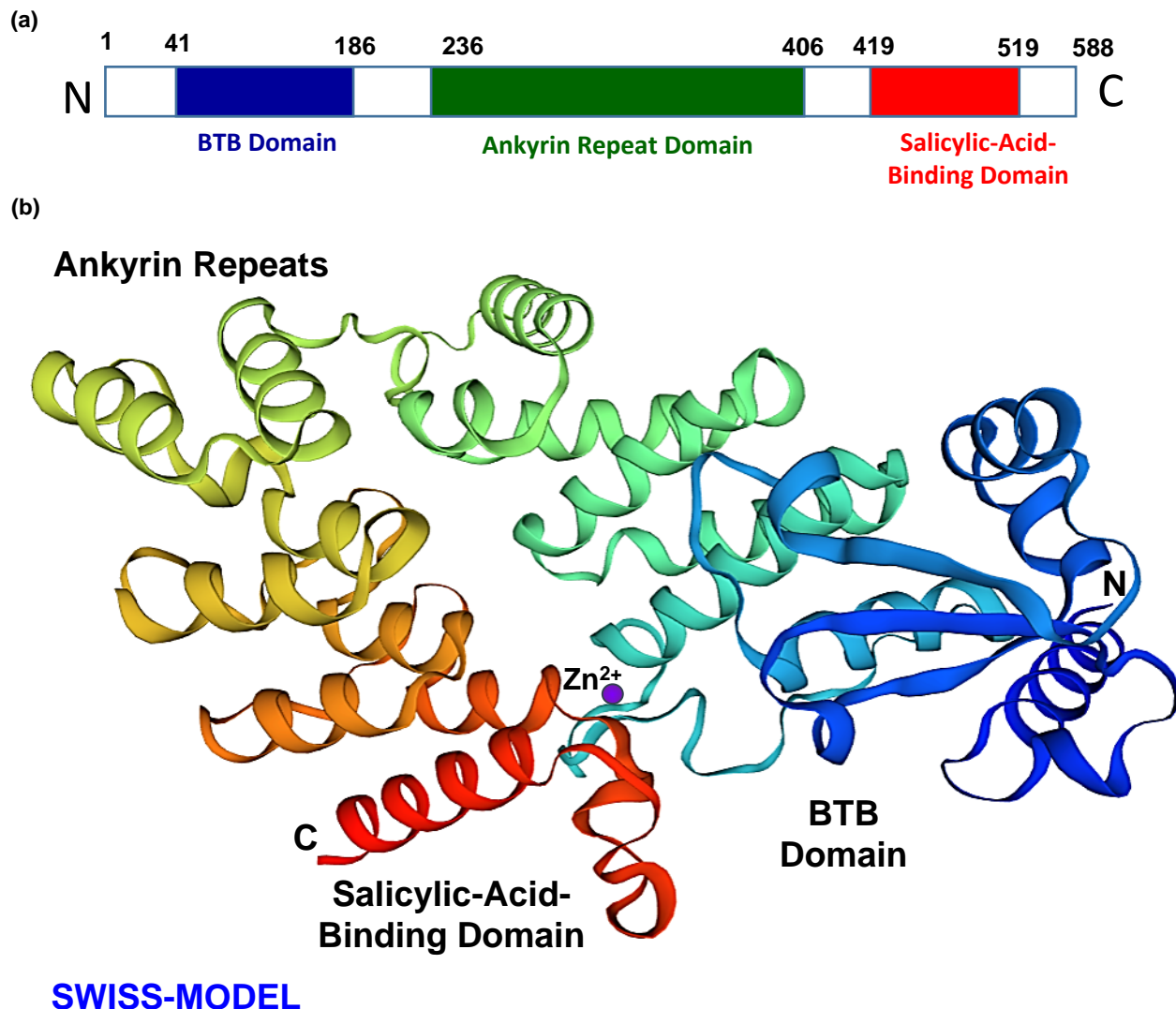


Figure S9. Information of functional domains and homology model NPR1 protein from *Nicotiana tabacum* (NtNPR1, KY402167) for functional analysis. (a) Domain map of the NtNPR1 protein to BTB domain, ankyrin repeats domain, and salicylic acid-binding domain using InterProScan for identifying the functional domains and protein families. (b) An NtNPR1 homology model (43–405 aa) was created with SWISS-MODEL at the highest score of global model quality estimate with the CryoEM structure of *Arabidopsis* NPR1.

Figure S10

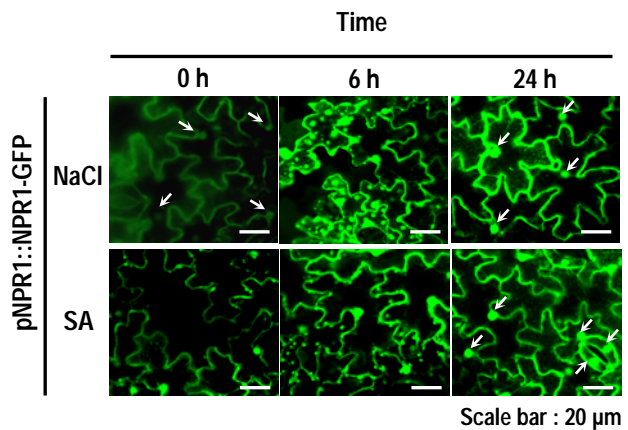


Figure S10. GFP fluorescence in the chloroplasts and nucleus of *p35S::cTP-NPR1-GFP* transgenic tobacco plants under salt stress. GFP-tagged nonexpressor of pathogenesis-related gene 1 (NPR1-GFP) localization in the pavement cells of abaxial leaf epidermis in *pNPR1::NPR1-GFP* transgenic plants under salt stress (upper) and salicylic acid (SA) treatment (middle) and *p35S::cTP-NPR1-GFP* transgenic plants under salt stress (lower). Arrows indicate NPR1 condensates.

Figure S11

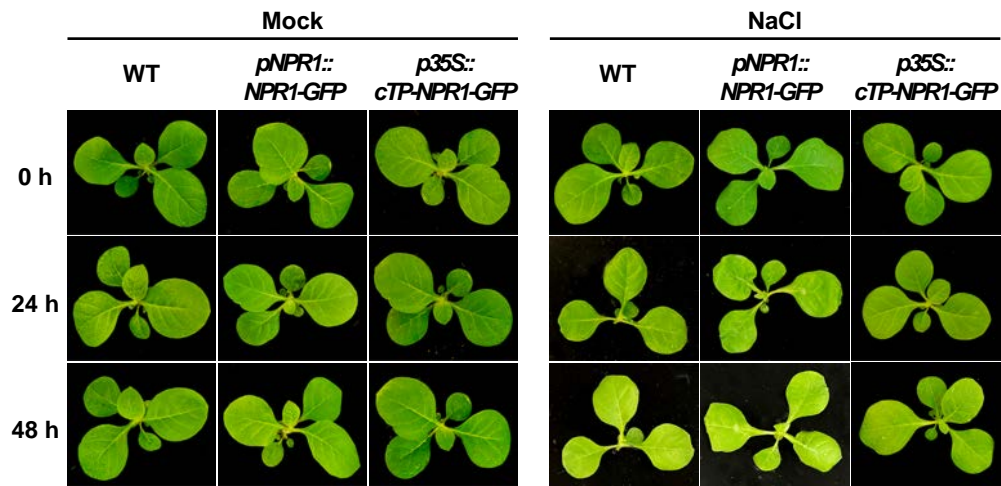
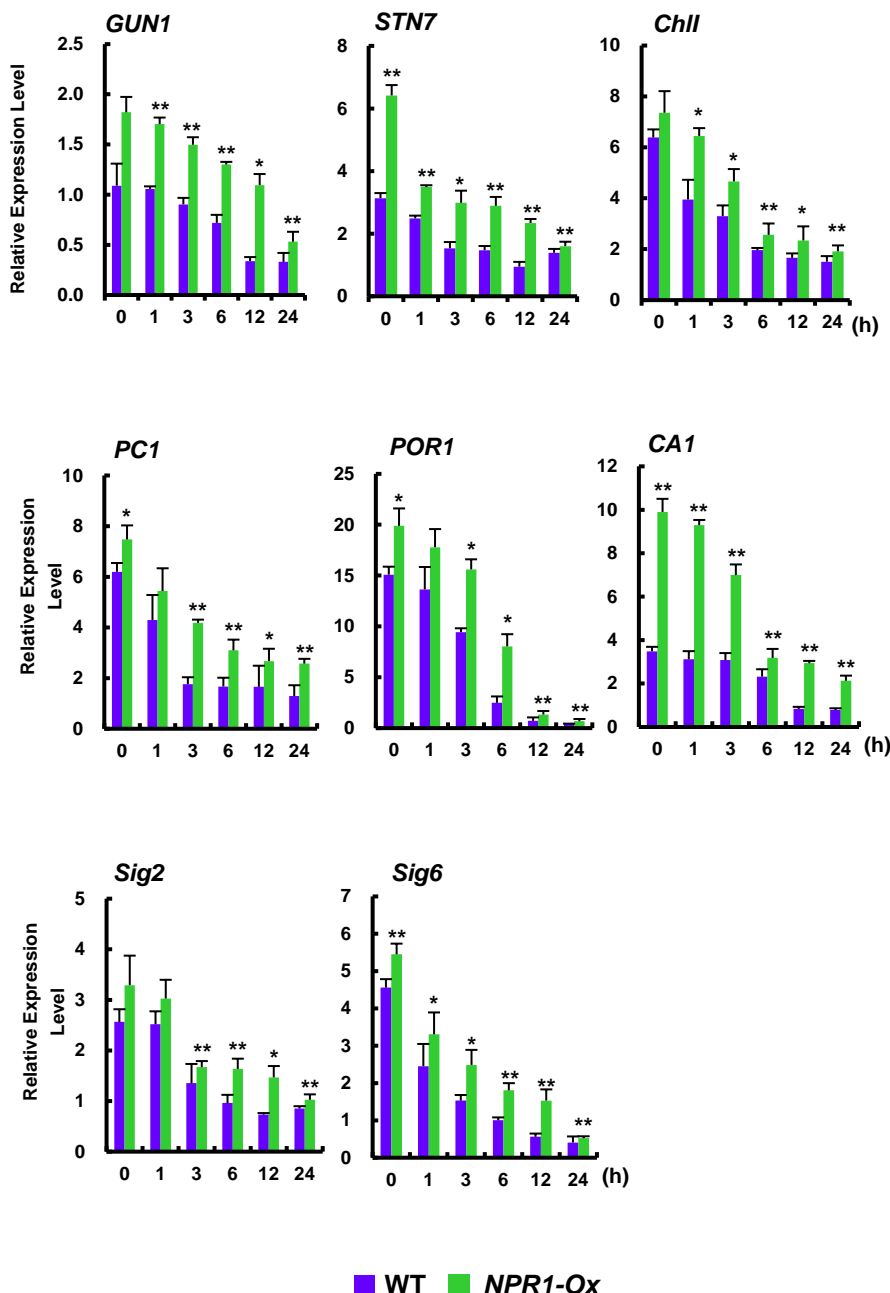


Figure S11. Phenotypes of WT and two transgenic tobacco lines under salt stress. Whole tobacco plants (WT, *pNPR1::NPR1-GFP*, and *p35S::cTP-NPR1-GFP*) were exposed to salt stress for 48 h.

Figure S12

(a)



■ WT ■ *NPr1-Ox*

(b)

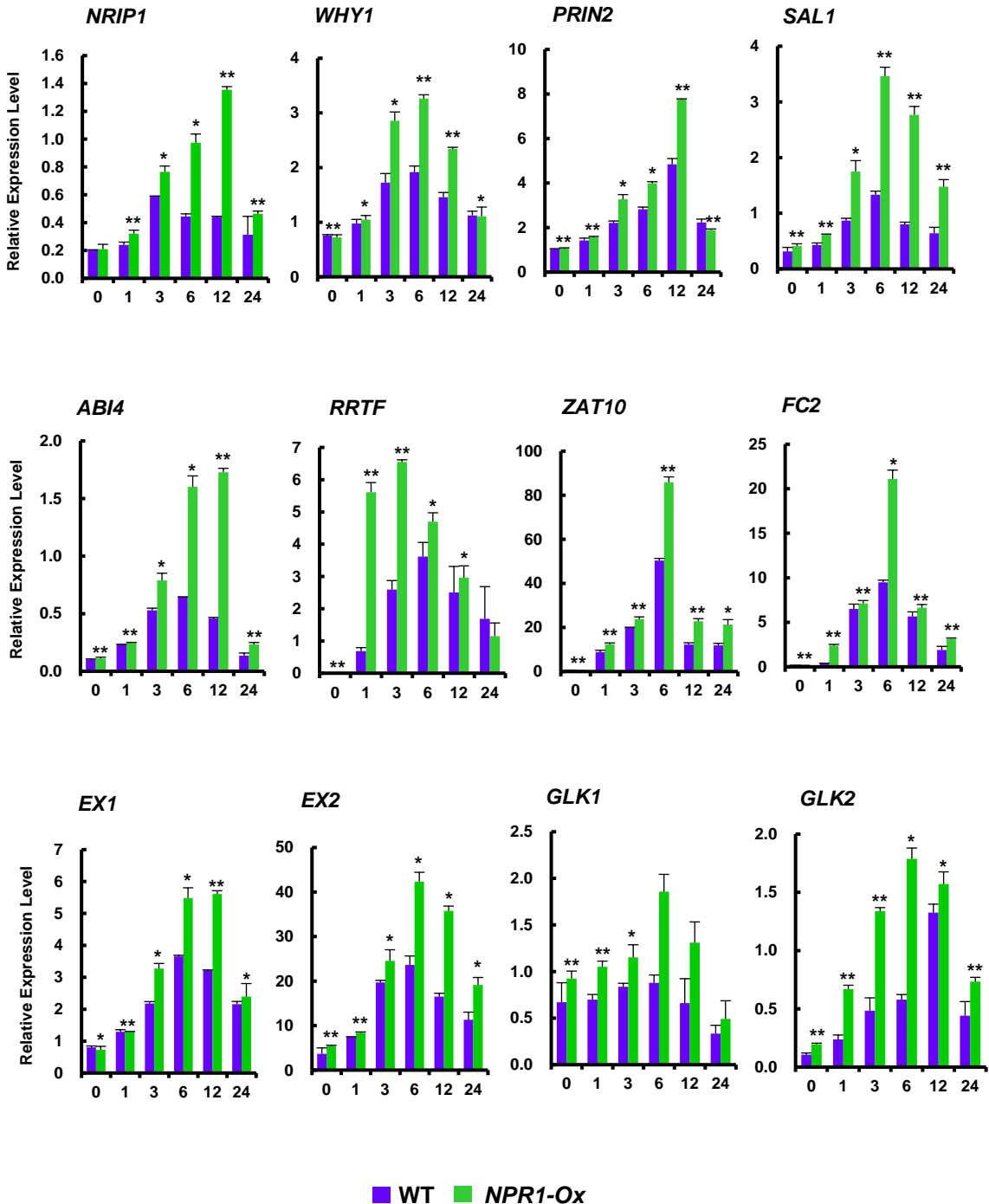


Figure S12. Transcription of retrograde signaling-related genes involved in chloroplast development and abiotic/biotic stress response in WT and *NPR1* overexpression (*NPR1-Ox*) transgenic tobacco plants under salt stress. Transcription profiles were determined using qRT-PCR in response to salt stress with 200 mM NaCl in WT and *NPR1-Ox* transgenic plant leaves and expressed relative to that of the reference gene β -actin. **(a)** Genes related to retrograde communication for chloroplast development: *GUN1*, genomes uncoupled1; *STN7*, serine/threonine-protein kinase7; *Chl1*, magnesium–protoporphyrin chelatase subunit; *PC1*, plastocyanin; NADPH:*POR1*, protochlorophyllide oxidoreductase; *CA1*, carbonic anhydrase 1; *Sig2*, chloroplast sigma factor 2; *Sig6*, chloroplast sigma factor 6. **(b)** Genes related to retrograde communication for operational signaling in response to biotic/abiotic stress: *NRIP1*, chloroplast NB-LRR receptor-interacting protein 1; *WHY1*, single-stranded DNA-binding protein WHIRLY 1; *PRIN2*, plastid redox insensitive 2; *SAL1*, 3'-phosphoadenosine 5'-phosphate (PAP) phosphatase; *ABI4*, abscisic acid-insensitive protein 4; *RRTF*, redox-responsive transcription factor; *ZAT10*, zinc-finger transcription factor 10; *FC2*, ferrochelatase; *EX1*, executer1; *EX2*, executer2; *GLK1*, golden 2-like1; *GLK2*, golden 2-like 2. Relative transcript expression levels are presented as mean \pm SD. Asterisks indicate significant differences between the WT and transgenic plants in each case (* $P<0.05$ or ** $P<0.01$).

Figure S13

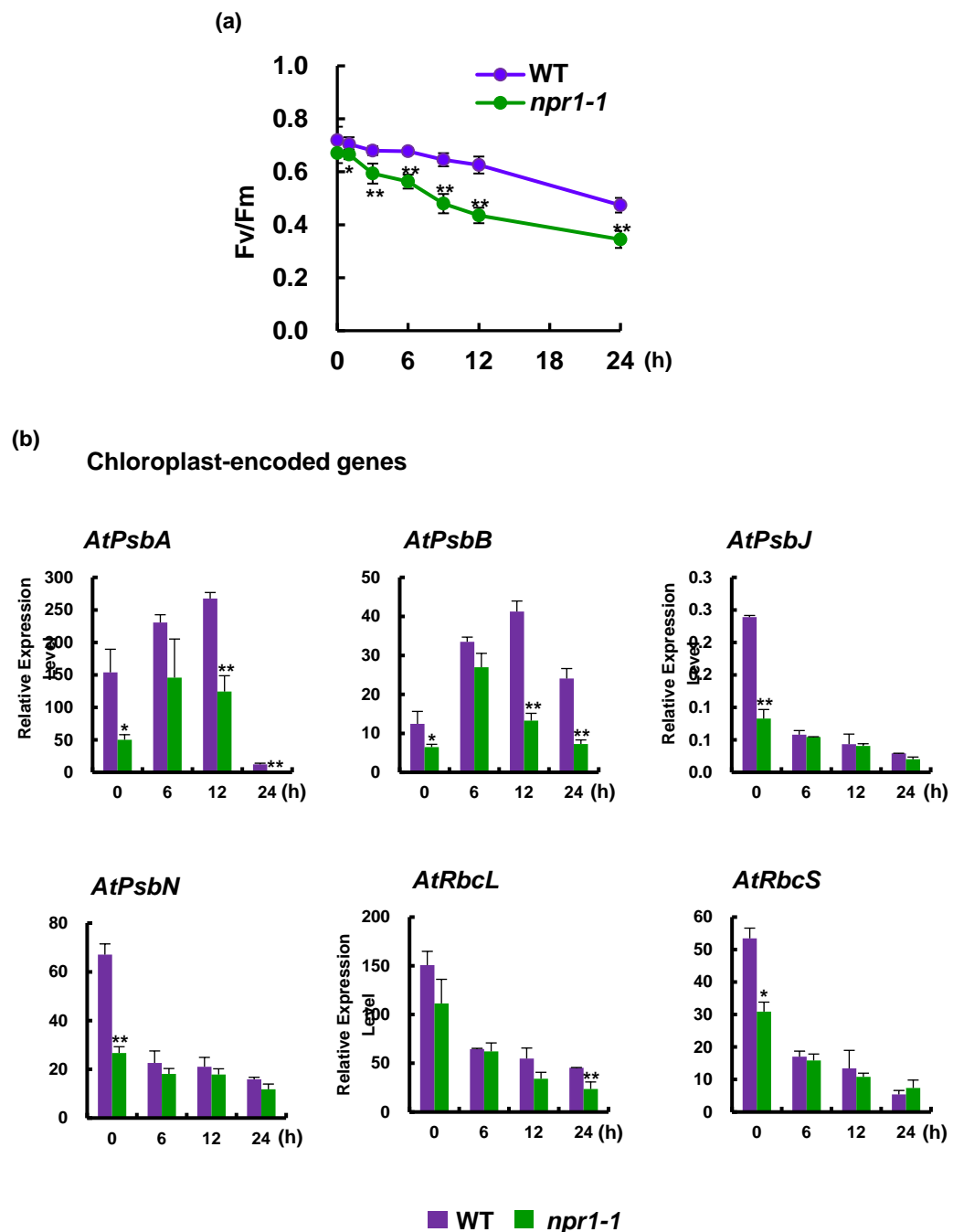


Figure S13. Kinetics of maximal photochemical efficiency and chloroplast-encoded gene transcription in WT and *npr1-1* mutant *Arabidopsis* plants under salt stress. **(a)** Maximal photochemical efficiency of photosystem II (PC II) (Fv/Fm) was measured in WT and *npr1-1* mutant *Arabidopsis* plants under salt stress. Fv/Fm values are expressed as mean \pm SD. **(b)** Transcription levels in WT and *npr1-1* mutant *Arabidopsis* plants in response to 200 mM NaCl-induced salt stress were measured using qRT-PCR and expressed relative to that of the reference gene β -actin. Chloroplast-encoded genes: *AtPsbA*, photosystem II reaction center D1 protein; *AtPsaB*, *AtPsbJ*, PC II reaction center protein J; *AtPsbN*, PC II subunit; *AtRbc L*, RuBisCo large subunit; *AtRbc S*, RuBisCo small subunit. Relative transcript expression levels are presented as mean \pm SD. Asterisks indicate significant differences between WT and *npr1-1* mutant *Arabidopsis* plants at the indicated time points (* $P<0.05$ or ** $P<0.01$).

Figure S14

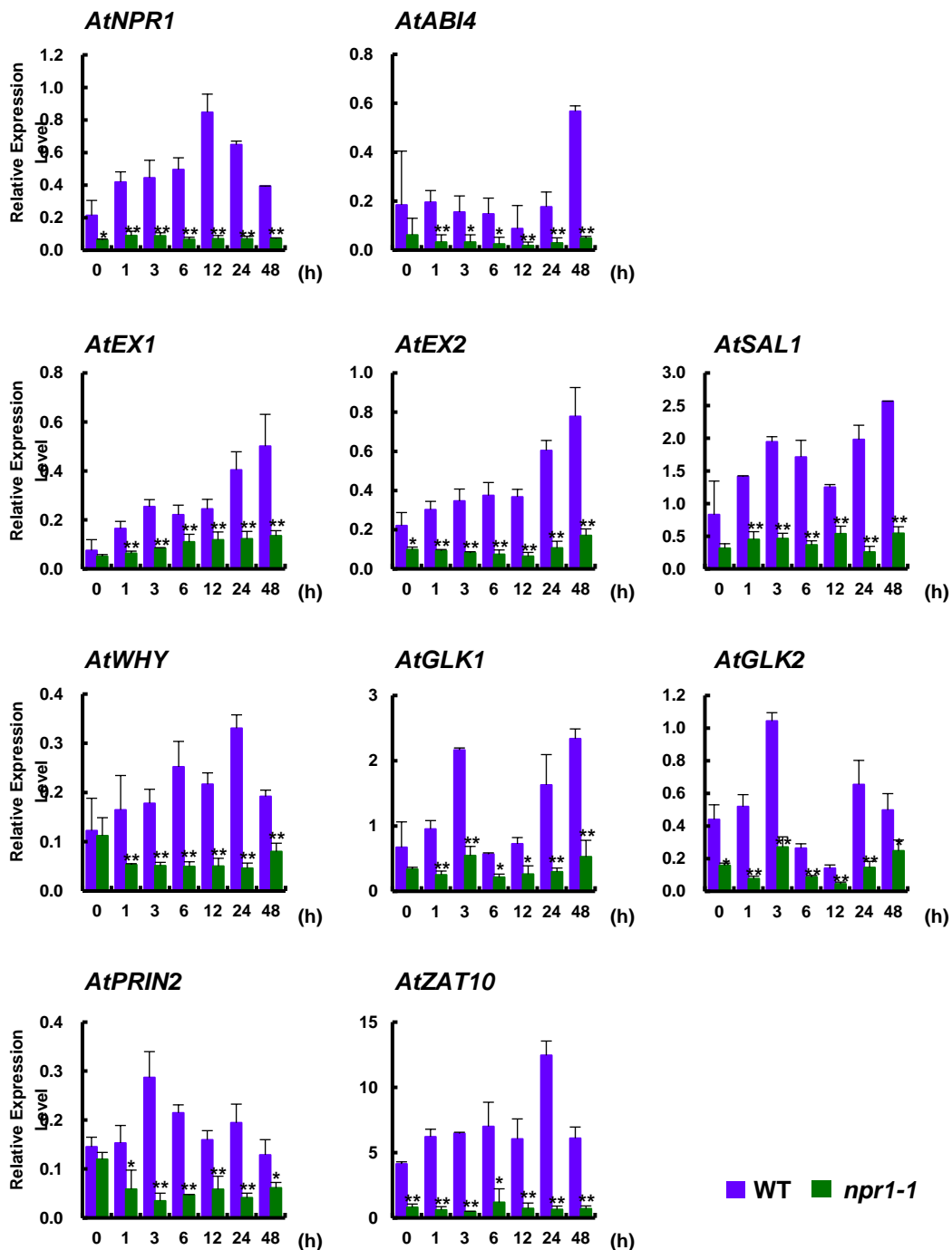


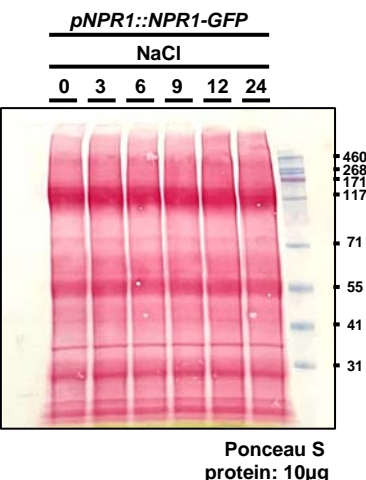
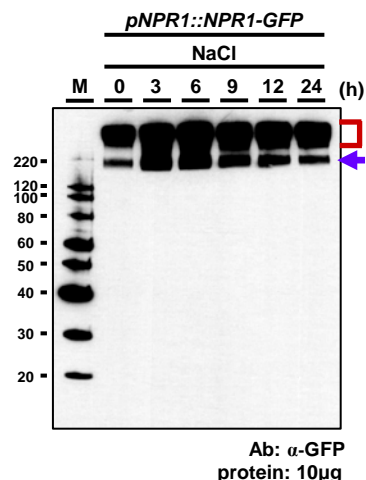
Figure S14. Transcription of retrograde signaling-related genes in response to abiotic/biotic stress in *Col-0* WT and *npr1-1* mutant *Arabidopsis* plants under salt stress. Transcription profiles in the leaves of WT and *npr1-1* mutants in response to 200 mM NaCl-induced salt stress were determined using qRT-PCR and expressed relative to that of the reference gene β -actin. Genes related in retrograde communication for operational signaling in response to biotic/abiotic stress: *AtNPR1*, nonexpressor of pathogenesis-related genes 1; *AtABI4*, abscisic acid-insensitive protein 4; *AtEX1*, executer1; *AtEX2*, executer2; *AtSAL1*, 3'-phosphoadenosine 5'-phosphate (PAP) phosphatase; *AtWHY1*, single-stranded DNA-binding protein WHIRLY 1; *AtGLK1*, golden 2-like1; *AtGLK2*, golden 2-like 2; *AtPRIN2*, plastid redox insensitive 2; *AtZAT10*, zinc-finger transcription factor 10. Relative transcript expression levels are presented as mean \pm SD. Asterisks indicate significant differences between WT and *npr1-1* mutant *Arabidopsis* plants at the indicated time points (* $P<0.05$ or ** $P<0.01$).

Supplementary materials

The full scan of the entire original blots

The full scan of the entire original blots: Figure 1A

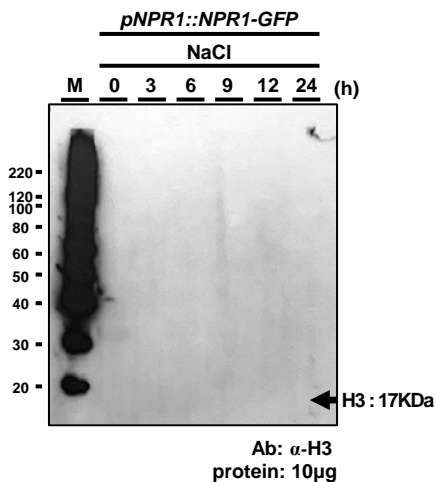
Chloroplast



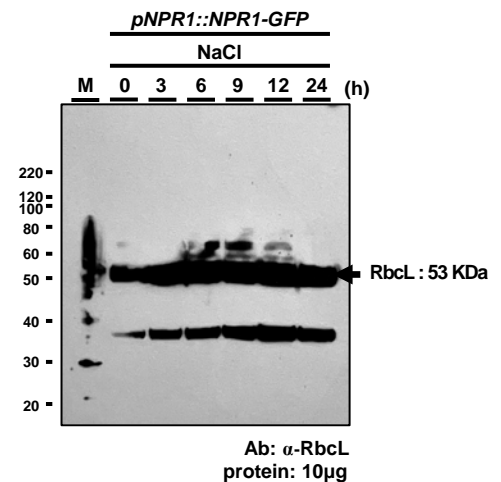
Relative Intensity

oligomer	1.0	1.6	1.5	1.4	1.4	1.1
dimer	1.0	2.8	2.6	2.1	1.8	1.1

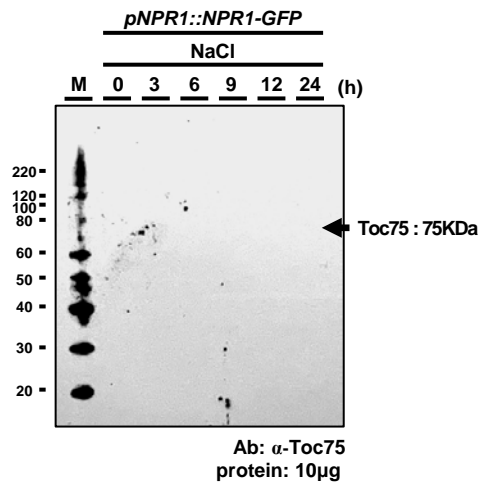
Nuclear marker: anti-Histon H3 antibody



Chloroplast stroma protein marker: anti-RbcL antibody

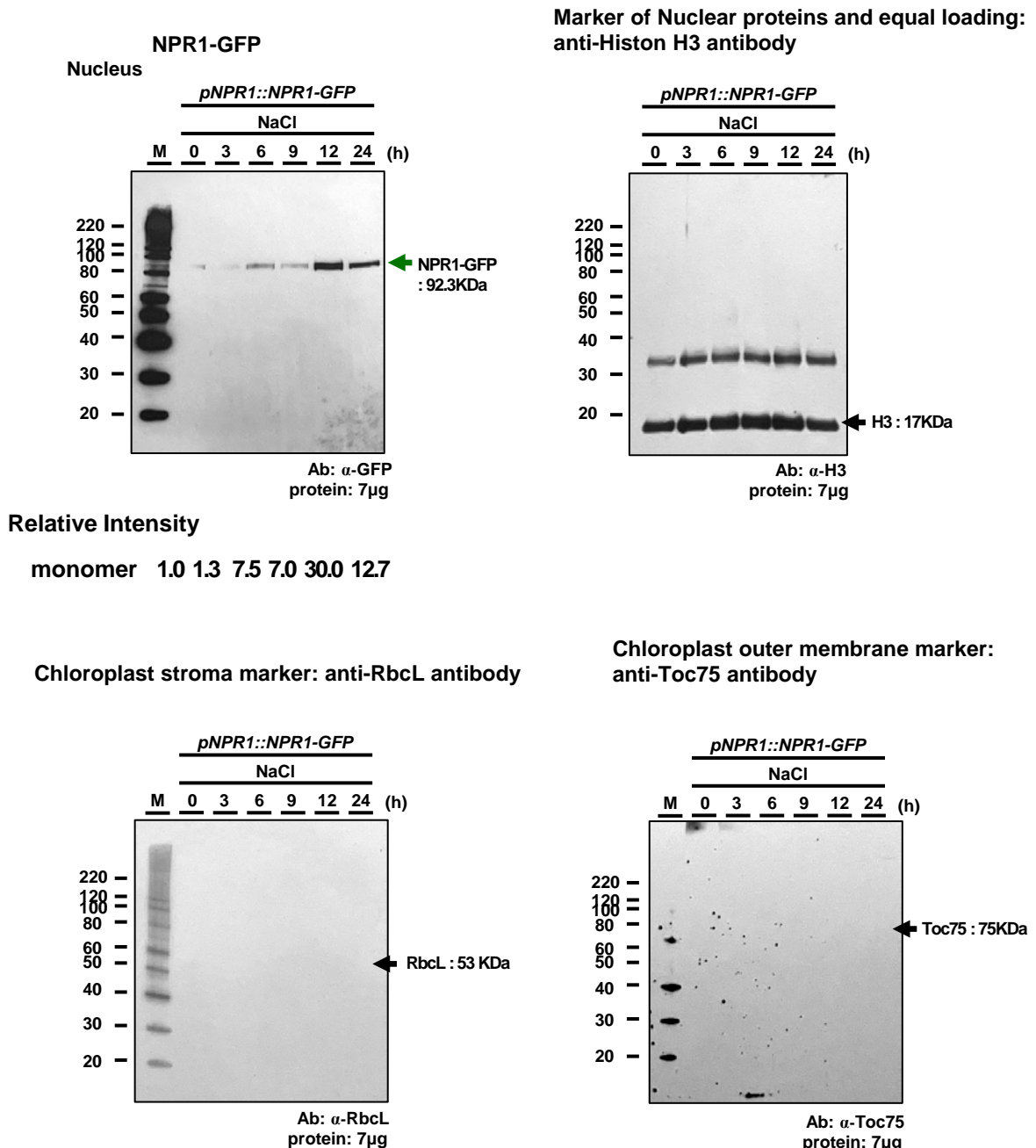


Chloroplast outer membrane marker: anti-Toc75 antibody



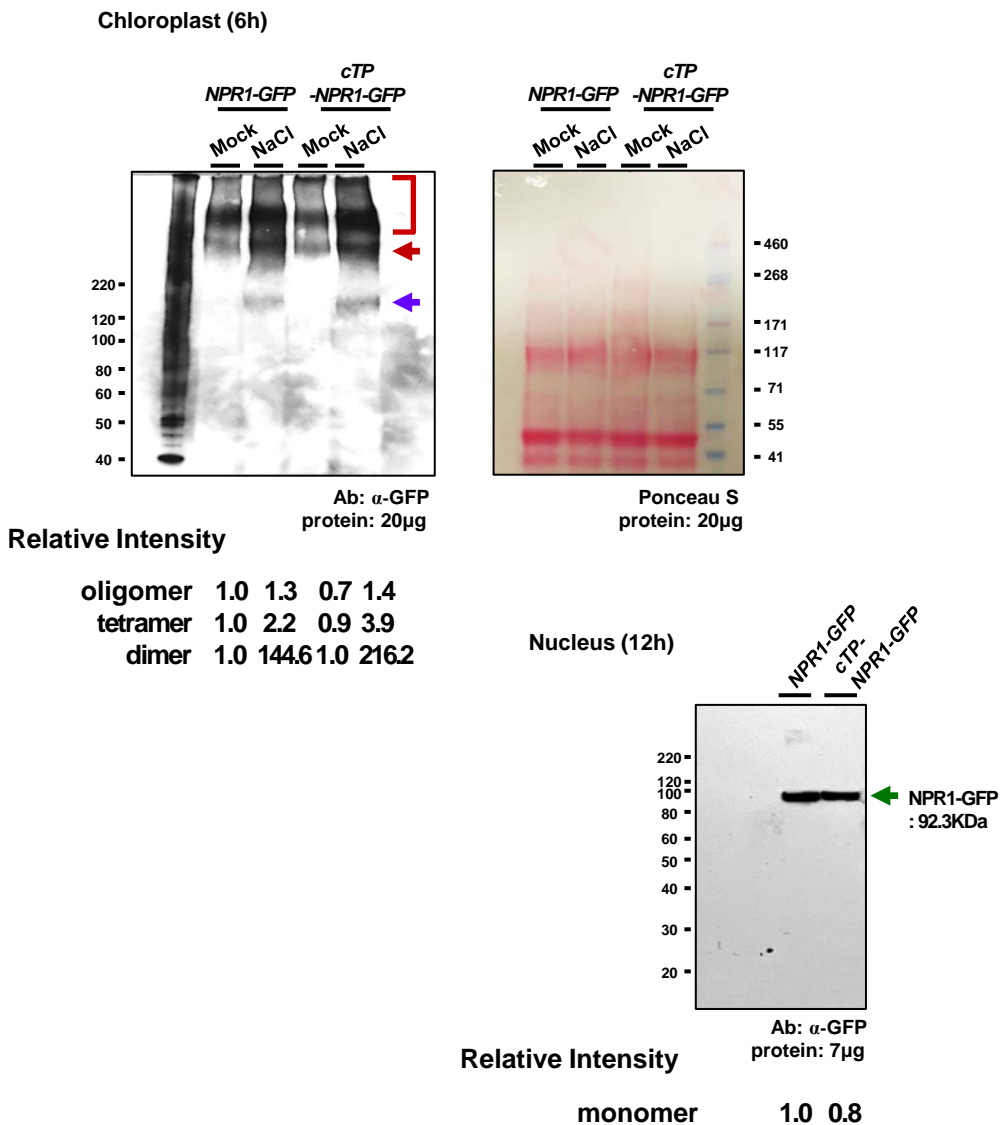
To ensure the reliability of our results, all experiments were repeated at least three times. Data from representative experiments were then reported after confirming consistency in the obtained results. To quantify band intensities, we utilized Image J software. Relative intensity was calculated by normalizing the band intensity values to the 0-hour treatment, which was assigned as 1.0.

The full scan of the entire original blots: Figure 1B



To ensure the reliability of our results, all experiments were repeated at least three times. Data from representative experiments were then reported after confirming consistency in the obtained results. To quantify band intensities, we utilized Image J software. Relative intensity was calculated by normalizing the band intensity values to the 0-hour treatment, which was assigned as 1.0.

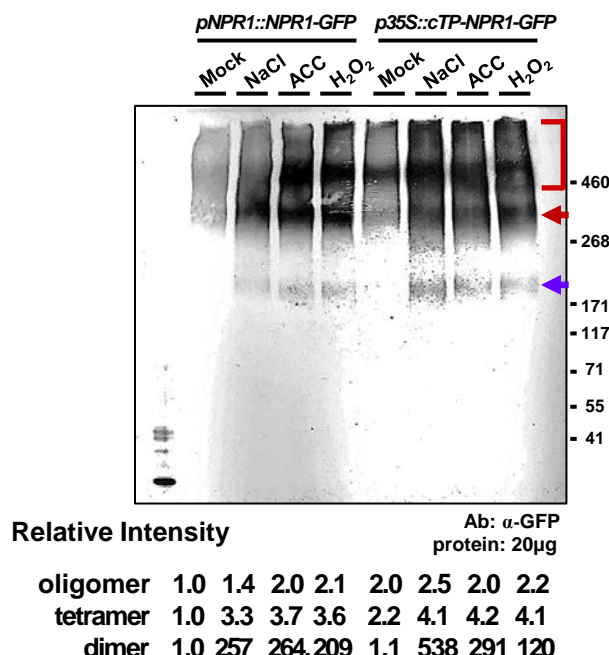
The full scan of the entire original blots: Figure 1D



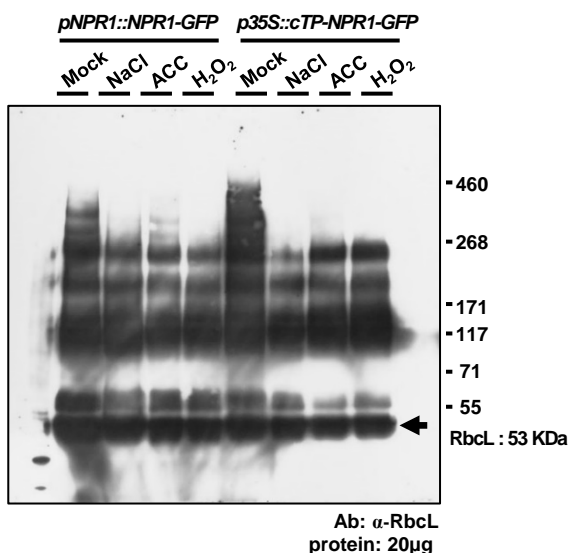
To ensure the reliability of our results, all experiments were repeated at least three times. Data from representative experiments were then reported after confirming consistency in the obtained results. To quantify band intensities, we utilized Image J software. (left) Relative intensity was calculated by normalizing the band intensity values to the mock treatment of *pNPr1::NPr1-GFP*, which was assigned a value of 1.0. (right) Relative intensity of *p35S::cTP-NPr1-GFP* was calculated by normalizing the band intensity values to *pNPr1::NPr1-GFP*, which was assigned as 1.0.

The full scan of the entire original blots: Figure 1G and 1J

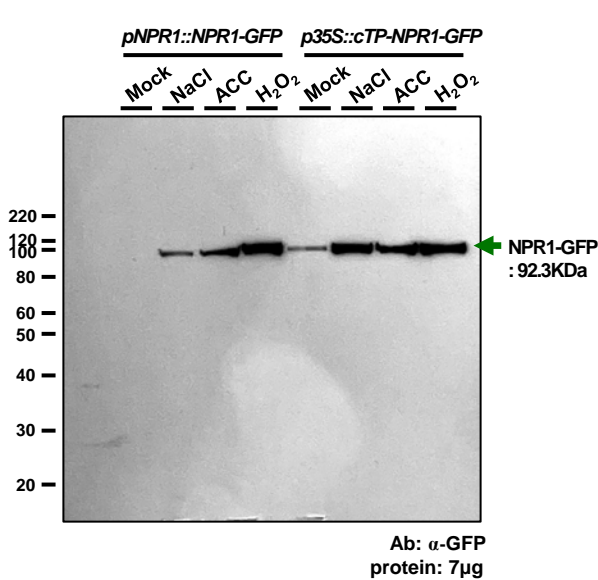
Chloroplast



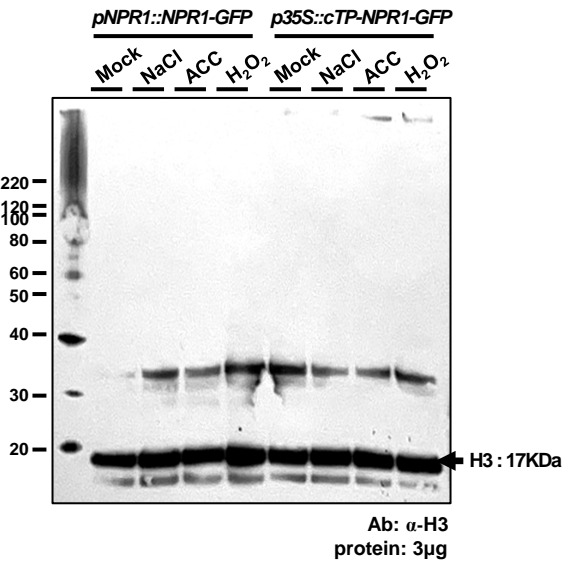
Marker of chloroplast stroma proteins : anti-RbcL antibody



Nucleus

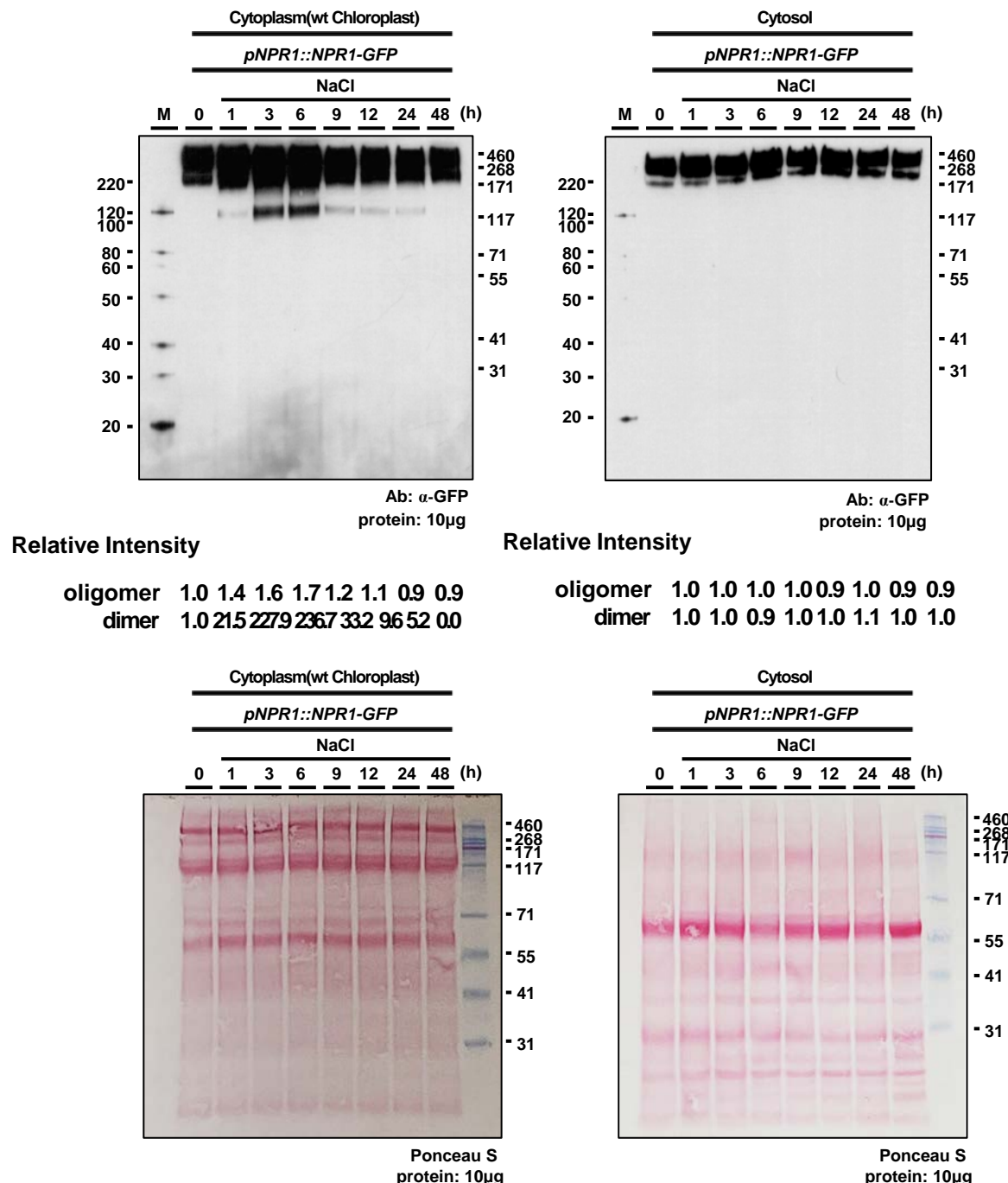


Marker of nuclear proteins and Equal loading:
anti-Histon H3 antibody



To ensure the reliability of our results, all experiments were repeated at least three times. Data from representative experiments were then reported after confirming consistency in the obtained results. To quantify band intensities, we utilized Image J software. Relative intensity was calculated by normalizing the band intensity values to the mock treatment of *pNPR1::NPR1-GFP*, which was assigned as 1.0.

The full scan of the entire original blots: Figure 3D



To ensure the reliability of our results, all experiments were repeated at least three times. Data from representative experiments were then reported after confirming consistency in the obtained results. To quantify band intensities, we utilized Image J software. Relative intensity was calculated by normalizing the band intensity values to the 0-hour treatment, which was assigned as 1.0.